Acta Polytechnica CTU Proceedings **37**:1–9, 2022
https://doi.org/10.14311/APP.2022.37.0001

Published by the Czech Technical University in Prague

SUBSALS: A SUBCHANNEL THERMAL-HYDRAULIC CODE FOR IRT TYPE FUEL ANALYSIS

Tomáš Adámek[a, b]

[a] *Czech Technical University in Prague, Faculty of Nuclear Sciences an Physical Engineering, Department of Nuclear Reactors, Břehová 7, 115 19 Prague, Czech Republic*

[b] *Research Centre Řež, Hlavní 130, Husinec-Řež, Czech Republic*

correspondence: tomas.adamek@cvrez.cz

Abstract. The LVR-15 research reactor is operated with a tube type fuel IRT-4M. Due to fuel's unique concentric square annular shape with, coolant flow is subject to significant pressure driven crossflow. Detailed calculation of such flow patterns is beyond capabilities of standard system codes used for the thermal hydraulic safety analysis. To assess safety of core designs consisting of the IRT-4M fuel assemblies, a new subchannel code is under development at Research Centre Řež and Czech Technical University in Prague.

Computer program SUBSALS is single phase, steady state, subchannel solver in development. Rigid computational mesh describes IRT-like geometries, and it is also suitable for other specific doubly connected ducts.

In this contribution, general description of calculation procedure and computational capabilities is presented along with code-to-code comparison. It could be used as proof of concept for future improvements in thermal hydraulic calculations of research reactors.

Keywords: SUBSALS, subchannel analysis, thermal-hydraulics, IRT-4M, LVR-15, crossflow.

1. Introduction

Thermal-hydraulic analysis of nuclear reactors is a necessary part of safety assessment. To maintain the integrity of physical barriers during the operation, appropriate cooling of all fuel assemblies must be ensured. Various sophisticated computational tools have been developed for the simulation of water cooled reactors behaviour.

Over the past decades increasing computational power of the computers allowed for a great development of one-dimensional system codes. Nuclear reactor core thermal-hydraulic safety assessment based on a hot channel theory, adopted to use in system codes, may be unnecessarily conservative. A more realistic approach to evaluate a core performance is accomplished using the subchannel analysis techniques. Computational models can be used to represent either an entire core or an individual sub-assembly.

The subchannel approach has been used extensively in light water reactor applications. It provides a higher degree of resolution than traditional system code approach and allows for a fast calculation of the flow, temperature, and void distributions with a reasonable accuracy.

Main domain of application of the traditional subchannel codes like SubChanFlow are core designs consisting of the rod bundles. Moreover, the efforts are made to develop advanced computational tools for the thermal-hydraulic analysis of the reactors operated with plate type fuel. For the utilization in reactors using tube type fuel, especially with significant pressure driven crossflow, however, modelling capabilities of the standard thermal-hydraulic simulation tools are limited.

2. General Description of the Subchannel Solver SUBSALS

Computer program SUBSALS (Subchannel Square Annular Layout Solver) is a single phase, steady state subchannel solver under development at Research Centre Řež and Czech Technical University in Prague. Its main purpose is the thermal-hydraulic analysis of the LVR-15 research reactor, which main goal is to determine cladding temperature distribution in the IRT-4M fuel assemblies under the normal operation.

2.1. IRT Type Fuel and Computational Mesh

The IRT type fuel is a series of sandwich, tube-type fuel assemblies with a square cross section, originally designed in 1963 as the IRT-M consisting of three fuel tubes. Later, further improvements in the fabrication process were achieved which led to four tube design IRT-2M. In 1979 a new generation, the IRT-3M was developed with an enhanced heat transfer area. Finally in 2004, the IRT-4M (Figure 1) design motivated by the RERTR program was completed [1].

Currently the IRT type fuel is used in two research reactors in Czech Republic (LVR-15 and VR-1), two research reactors in Russia (IR-8 and IRT-T) and one research reactor in Uzbekistan (VVR-SM) [2].

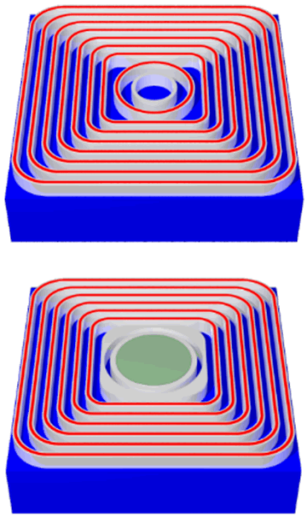

Figure 1. Geometry of the IRT-4M fuel assemblies: standard 8-tube fuel assembly (top) and control 6-tube fuel assembly (bottom) [3].

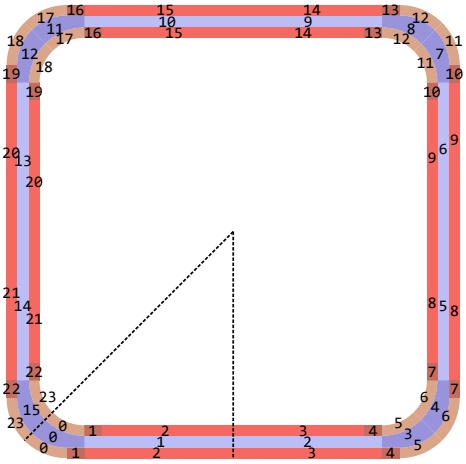

Figure 2. Radially-azimuthal view of the computational mesh.

In it's current state of development, for the sake of modularity, SUBSALS is designed to analyse one coolant channel between the fuel tubes. The interaction between multiple coolant channels will be achieved by the external iterator module in later stages of development.

The computational mesh (Figure 2) is rigid in radial and azimuthal direction and user defined in axial direction. Radially one coolant channel azimuthally divided into 16 unique subchannels is presented surrounded from both sides by fuel tubes, both azimuthally divided into 24 unique fuel elements.

2.2. Basic Conservation Equations

Due to multiple simplifications in presented problem and lack of experimental data for precise validation on various specific phenomena, SUBSALS code uses a simple marching procedure as described in [4]. Combination of the rigid radially-azimuthal computational mesh and the marching procedure makes it possible to use a third-party numerical solver. GNU Scientific Library (GSL) [5] is implemented in the program to solve a non-linear systems of the conservation equations, hence no linearization of the equations is needed.

For an axial node n for the subchannel i the basic conservation equations in finite difference form are the following.

Mass Conservation:

$$\begin{aligned} 0 \equiv & \frac{S_i}{\Delta z}\left(\rho_i^n w_i^n - \rho_i^{n-1} w_i^{n-1}\right) \\ & + W^n_{i\to(i-1)} \\ & + W^n_{i\to(i+1)}, \end{aligned} \tag{1}$$

where S is subchannel flow area, Δz is length of axial node, ρ is water density, w is water velocity, $W_{x\to y}$ is diversion crossflow from subchannel x to subchannel y.

Energy Conservation:

$$\begin{aligned} 0 \equiv & \frac{S_i}{\Delta z}\left(\rho_i^n w_i^n h_i^n - \rho_i^{n-1} w_i^{n-1} h_i^{n-1}\right) \\ & - {}_{\text{lin.}}q_i^n \\ & + w'^n_{i\to(i-1)}\left(h_i^n - h_{i-1}^n\right) \\ & + w'^n_{i\to(i+1)}\left(h_i^n - h_{i+1}^n\right) \\ & + W^n_{i\to(i-1)} h^{*n}_{i-1} \\ & + W^n_{i\to(i+1)} h^{*n}_{i+1}, \end{aligned} \tag{2}$$

where h is specific enthalpy of water, ${}_{\text{lin.}}q$ is linear heat rate transferred to subchannel, $w'_{x\to y}$ is turbulent crossflow from subchannel x to subchannel y, h^* is specific enthalpy of water in donor subchannel.

Axial Momentum Conservation:

$$\begin{aligned} 0 \equiv & \frac{S_i}{\Delta z}\left(\rho_i^n \left(w_i^n\right)^2 - \rho_i^{n-1}\left(w_i^{n-1}\right)^2\right) \\ & + \mathcal{F} w'^n_{i\to(i-1)}\left(w_i^n - w_{i-1}^n\right) \\ & + \mathcal{F} w'^n_{i\to(i+1)}\left(w_i^n - w_{i+1}^n\right) \\ & + W^n_{i\to(i-1)} w^{*n}_{i-1} \\ & + W^n_{i\to(i+1)} w^{*n}_{i+1} \\ & + \rho_i^n g S_i \\ & + \frac{S_i}{\Delta z}\left(p_i^n - p_i^{n-1}\right) \\ & + \frac{1}{2}\frac{f_i^n}{d_{\text{h}i}} \rho_i^n S_i \left(w_i^n\right)^2, \end{aligned} \tag{3}$$

where $\mathcal{F}$ is correction factor to help account for the difference between energy and momentum turbulent transport, g is acceleration due to gravity, p is water pressure, f is Darcy-Weisbach friction factor, d_{h} is hydraulic diameter of subchannel, w^* is water velocity in donor subchannel.

Transverse Momentum Conservation:

$$0 \equiv \frac{s_{i\to(i-1)}}{l_{i\to(i-1)}}\left(p_i^n - p_{i-1}^n\right) + \frac{K_{\text{trans.}}\left|W_{i\to(i-1)}\right| W_{i\to(i-1)}}{2\left(s_{i\to(i-1)}\right)^2 \rho^{*n}_{i-1}} \frac{s_{i\to(i-1)}}{l_{i\to(i-1)}}, \quad (4)$$

where $s_{x\to y}$ is effective width of control volume for transversal flow from subchannel x to subchannel y, $l_{x\to y}$ is effective length of control volume for transversal flow from subchannel x to subchannel y, ρ^* is density of water in donor subchannel, $K_{\text{trans.}}$ is transverse flow pressure loss coefficient.

2.3. Constitutive Equations

To solve the conservation equations, a state equation is needed to obtain thermophysical properties of water. For this purpose the external CoolProp [6] library for calculation of the thermodynamic properties of water and steam in form of IAPWS-IF97 formulation is used.

Beside the physical properties,a power distribution, constitutive relations and boundary conditions are needed to avoid underdetermination of the system of equations.

Boundary conditions, as well as power profile, are implemented via user's inputs. The power distribution is assumed to be spatially separable, hence total heat P_i transferred to coolant from fuel element i is

$$P_i = P_0 \phi_i^{\text{rad.}} \phi_i^{\text{az.}} \phi_i^{\text{ax.}} \vartheta, \quad (5)$$

where P_0 is total power generated in fuel assembly. Coefficients $\phi_i^{\text{rad.}}, \phi_i^{\text{az.}}, \phi_i^{\text{ax.}}$ are normalized relative powers of fuel element i in radial, azimuthal and axial direction. Coefficient ϑ denotes fraction of the heat transferred to the coolant from whole fuel tube, allowing not only to use adiabatic boundary condition $\vartheta \equiv 1$, but also the simple approximation of the uniform power split boundary condition $\vartheta \equiv 0.5$.

In the program SUBSALS, various correlations for the friction factor and the heat transfer coefficient calculation are implemented. Frictional pressure drop in turbulent regime is calculated using Darcy-Weisbach friction factor. Widely used formula proposed by Blasius [7] for calculation of the friction factor in hydraulically smooth pipes reads:

$$f = 0.3164\text{Re}^{-0.25}, \quad (6)$$

where Re is Reynolds number. To include a surface roughness ε in the calculation, Zigrang-Sylvester's approximation [8] to Colebrook-White correlation, is implemented as:

$$\frac{1}{\sqrt{f_{\text{t.}}}} = -2\log_{10}\left\{\frac{\varepsilon}{3,7 d_{\text{h}}} + \frac{2,51}{\text{Re}}\left[1,14 - 2\log_{10}\left(\frac{\varepsilon}{d_{\text{h}}} + \frac{21,25}{\text{Re}^{0,9}}\right)\right]\right\}, \quad (7)$$

which is the same form as implemented in the standard thermal-hydraulic codes, e.g. system code RELAP5/MOD3 [9] or subchannel code CTF [10].

Due to lack of experimental data, simplified models of various parameters from the conservation equations are used. Turbulent transport correction factor $\mathcal{F}$ is set to be zero, similarly as in an input example in [11]. This assumption makes turbulent mass transport effect on pressure equalization between subchannels negligible. Transverse flow pressure loss coefficient is set to be 0.5, as suggested in various textbooks similarly as in an input example in [11].

In the rod bundles, particular attention is paid to describe a turbulent crossflow mixing. Great review of the experimental studies and correlations on this topic is available in the study [12]. For a turbulent crossflow the simplest formula was implemented:

$$w'_{x\to y} = \beta s \bar{G}, \quad (8)$$

where $\bar{G}$ is an average mass flux of neighbouring subchannels x and y, β is turbulent factor. One of the most common formulae suggested in [12] for turbulent factor proposed by Beus reads:

$$\beta = 0.0035\text{Re}^{-0.1}\frac{\bar{d_{\text{h}}}}{s}, \quad (9)$$

where $\bar{d_{\text{h}}}$ is average hydraulic diameter of neighbouring subchannels x and y.

Cladding temperature of given fuel element is calculated using Newton's law:

$${}_{\text{surf.}}q = \alpha\left(T_{\text{clad.}} - T_\infty\right), \quad (10)$$

where ${}_{\text{surf.}}q$ is heat flux from given fuel element to adjacent subchannel, $T_{\text{clad.}}$ is cladding temperature, T_∞ is bulk water temperature in adjacent subchannel and α is heat transfer coefficient defined as:

$$\alpha = \frac{\text{Nu}\lambda_{\text{f}}}{d_{\text{h}}}, \quad (11)$$

where Nu is Nusselt number and λ_{f} is water conductivity. Heat transfer coefficient is function of Nusselt number, hence another constitutive relation is required.

Great review and validation of Nusselt number correlations for high aspect ratio rectangular geometry is available in the thesis [13]. Four different correlations for Nusselt number calculation are implemented in the program SUBSALS. One of the most commonly used correlations proposed by Dittus and Boelter [14] reads:

$$\text{Nu} = 0.023\text{Re}^{0.8}\text{Pr}^{0.4}, \quad (12)$$

where Pr is Prandtl number.

Another implemented correlation proposed by Popov and Petukhov [15] with Siman-Tov's correction for rectangular geometry as suggested in [13]:

$$\begin{aligned} \mathrm{Nu} &= \frac{\frac{1}{8} f \mathrm{RePr}}{K_1(f) K_2(\mathrm{Pr}) \sqrt{\frac{f}{8}} \left(\mathrm{Pr}^{\frac{2}{3}} - 1\right)} \\ K_1(f) &= (1 + 3.4f) \\ K_2(\mathrm{Pr}) &= \left(11.7 + 1.8\mathrm{Pr}^{-\frac{1}{3}}\right), \end{aligned} \tag{13}$$

where friction factor f is calculated using Filonenko:

$$f = \frac{1.0875 - 11.25\mathcal{A}}{1.82 \log_{10} \mathrm{Re} - 1.64^2}, \tag{14}$$

where $\mathcal{A}$ is subchannel aspect ratio.

From Popov-Petukhov correlation, Gnielinski [13] obtained another formula, which is often regarded as one of the most accurate:

$$\mathrm{Nu} = \frac{0.5f\,(\mathrm{Re} - 1000)\,\mathrm{Pr}}{1 + 12.7\sqrt{0.5f}\left(\mathrm{Pr}^{\frac{2}{3}} - 1\right)}, \tag{15}$$

where friction factor is calculated according to formula:

$$f = (1.58 \ln \mathrm{Re} - 3.28)^{-2}. \tag{16}$$

Finally, correlation proposed by Sieder and Tate [13] is adopted:

$$\mathrm{Nu} = 0.027 \mathrm{Re}^{0.8} \mathrm{Pr}^{\frac{1}{3}}. \tag{17}$$

To account for the wall temperature effect on boundary layer, Nusselt number is multiplied by cladding temperature dependent correction factor throughout the iterative procedure. Different correction factors are used for individual correlations as listed below:

- Dittus-Boelter correlation is corrected by factor $\left(\frac{\mu_\infty}{\mu_{\mathrm{clad.}}}\right)^{0.11}$ as suggested by [15].
- Popov-Petukhov correlation is corrected by factor $\left(\frac{\mu_\infty}{\mu_{\mathrm{clad.}}}\right)^{0.11}$ as suggested by [15].
- Gnielinski correlation is corrected by factor $\left(\frac{\mu_\infty}{\mu_{\mathrm{clad.}}}\right)^{0.11}$ as suggested by [15].
- Sieder-Tate correlation is corrected by factor $\left(\frac{\mu_\infty}{\mu_{\mathrm{clad.}}}\right)^{0.14}$ as suggested by [13].

Similar correction of value $\left(\frac{\mu_{\mathrm{clad.}}}{\mu_\infty}\right)^{0.11}$ is used for friction factor [15].

3. Code-to-Code Comparison

According to the IAEA Safety Standards series [16] code validation should be performed on all computer codes that are used for the deterministic safety analysis of nuclear reactors. The purpose of code assessment is to provide confidence in the ability of a code to predict the values of parameters of interest and quantify the accuracy of prediction. The code qualification process should be based on the information from analytical solutions, experimental data, nuclear and benchmark calculations (code-to-code comparisons).

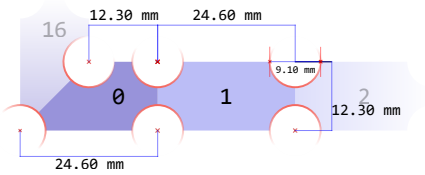

Figure 3. Radially-azimuthal view of the one-eighth of the pin type square annular geometry geometry (with adjacent subchannels).

To address basic verification, reference pin type square annular geometry (Figure 3) was proposed as the compromise between a standard subchannel code problem and limited modelling capabilities of the code SUBSALS. Geometry consists of 16 subchannels arranged to square annular shape and 32 fuel pins. Each subchannel is neighbouring with exactly two other subchannels. Using this geometry, a flow and temperature distribution in coolant can be compared using various boundary conditions described below. Throughout all test cases turbulent mixing was disabled.

3.1. Friction Flow Split

Using the geometry from Figure 3, basic flow split problem can be addressed. Due to the symmetry, only two subchannels, e.g. 0 and 1, are essentially needed to be examined. The inlet velocity is uniform in all subchannels, power is set to be zero, and water is highly subcooled. This initial conditions create a difference in frictional pressure drops in the two subchannels, which create a lateral pressure gradient. Flow is driven from the higher resistance subchannel to the lower resistance subchannel, hence the name diversion or pressure driven crossflow.

Flow distribution changes along the axial direction. Velocity increases in the low-resistance subchannel, which increases frictional pressure drop in that subchannel and vice versa. Flow exchange continues until the frictional pressure losses are equal in both subchannels and subchannels are in mechanical equilibrium. An analytical solution can be calculated for mechanical equilibrium point.

For friction flow split comparison, following boundary conditions were used:

- Inlet temperature is set to 50 °C.
- Outlet pressure is set to $1 \cdot 1.8 \cdot 10^5$ Pa.
- Inlet velocity is set to be 2, 3, 4 and 5 $\mathrm{m \cdot s^{-1}}$.

Typical axial velocity distribution comparison is shown in Figure 4. Results for the inlet velocities 2, 3, 4 and 5 m/s are presented in Table 1. These results demonstrate that SUBSALS predicts expected flow split in the PTSA-VER-1 geometry and axial velocity

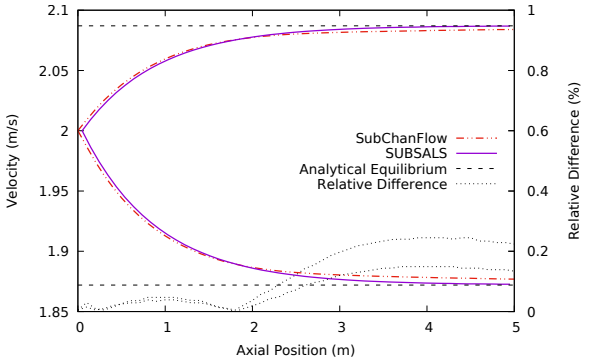

FIGURE 4. Comparison of axial velocity distribution calculation with analytical solution.

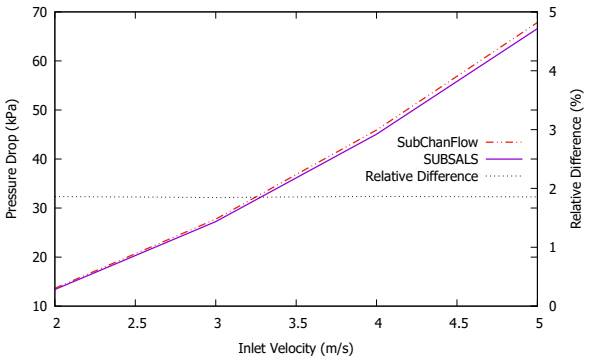

FIGURE 5. Comparison of pressure drop calculations.

Inlet Velocity [m·s^{-1}]	Maximal Error [%]		Analytical Equilibrium Error [%]	
	Ch. 0	Ch. 1	Ch. 0	Ch. 1
2	0.149	0.245	0.01	0.04
3	0.170	0.270	0.03	0.06
4	0.170	0.282	0.03	0.07
5	0.175	0.279	0.05	0.09

TABLE 1. Friction flow split comparison results.

distribution is in great agreement with SubChanFlow calculation.

3.2. Pressure Loss

Friction flow split calculations were also used to evaluate frictional pressure drops using both SUBSALS and SubChanFlow, see Figure 4. Comparison demonstrates that SUBSALS predicts frictional pressure loss in PTSA-VER-1 geometry consistently with SubChanFlow calculation.

3.3. Axial Temperature Profile and Cladding Temperature

One of the main tasks of each thermal-hydraulic code is to predict coolant enthalpy profile, and thus the temperature profile, under different power distribution boundary conditions. To compare cladding and water temperature profile computed using SUBSALS and SubChanFlow, four test cases were defined, all with uniform radially-azimuthal power profile:

(1.) Uniform axial power profile.

(2.) Linearly increasing axial power profile.

(3.) Linearly decreasing axial power profile.

(4.) Sine axial power profile.

Throughout all test cases turbulent mixing was disabled.

Results of water velocity, water temperature and cladding temperature distributions calculations were compared from both codes with uniform radially-azimuthal power profile, hence total heat-flux to each subchannel in individual axial nodes was the same. Other boundary conditions were unchanged from previous tests. Overall power transferred to coolant was set to 0.7 MW. A typical axial velocity distribution, axial cladding and water temperature distributions comparisons are shown in Figures 6, 7, 8 and 9. Calculations results are summarised in Table 2. Maximal pressure drop difference between corresponding calculations is 2.1 % with average error only 0.8 %.

3.4. Maximum Cladding Temperature

Maximum cladding temperature is one of the most important safety parameters, thus capability of subchannel code to correctly predict this value is of great importance. Furthermore, being independent on the axial nodalization inconsistency, peak cladding temperature is a valuable parameter for code-to-code comparison.

Maximal peak cladding temperature difference between both calculations is 1.02 °C, see Figure 10, which is significantly less than maximal cladding temperature error 2.23 °C. Almost all predictions of peak cladding temperature calculated using code SUBSALS are conservative, maximal non-conservative error being only 0.36 °C.

4. Conclusions and Outlook

In this work new subchannel thermal-hydraulic computer code for analysis of the light water research reactors operated with the IRT type fuel assemblies is presented. The main objective of this study is code-to-code comparison of the program SUBSALS against the standard validated subchannel code SubChanFlow using the reference test geometry.

Overall 19 different calculations divided into five groups of tests were performed with and without power, with different inlet velocities and different axial power profiles. It is shown, that SUBSALS code provides reasonable predictions of the coolant flow and enthalpy distribution, consistent with reference calculations provided by SubChanFlow. SUBSALS can predict pressure drop within ±2.5 % error from SubChanFlow calculations. Maximal coolant temperature and velocity RMSE is 0.54 °C and 0.020 m·s^{-1} respectively. Maximal cladding temperature RMSE

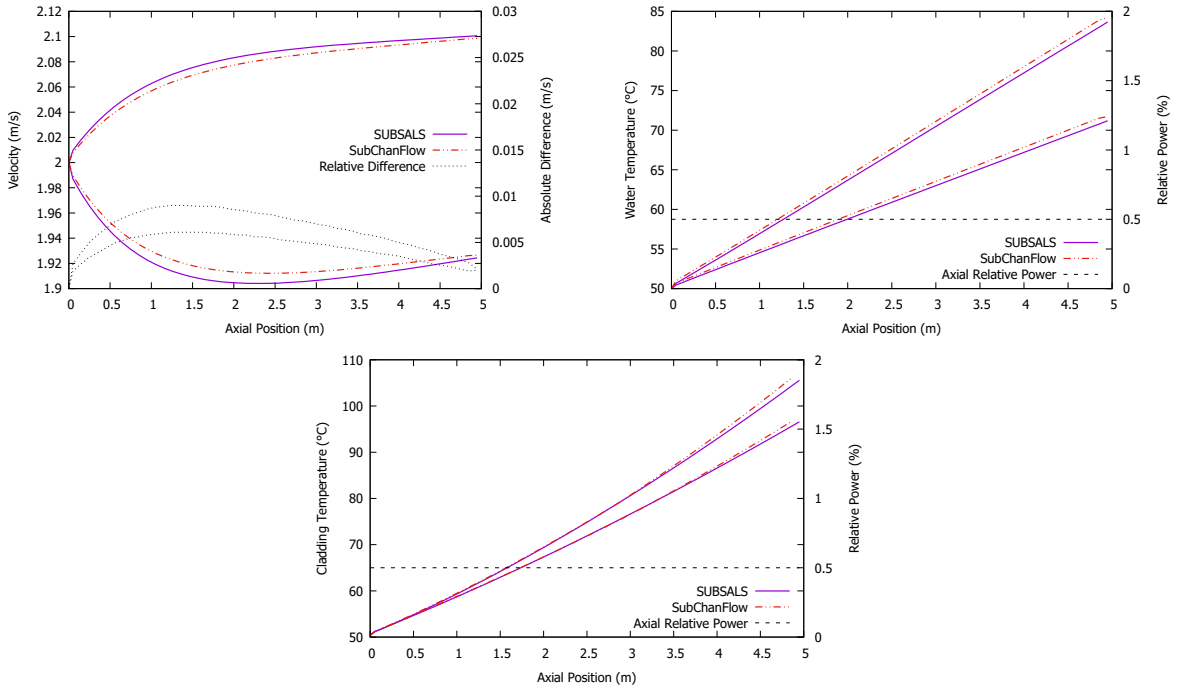

Figure 6. Comparison of axial velocity (top left), water temperature (top right) and cladding temperature (bottom) distribution calculations with uniform axial power distribution.

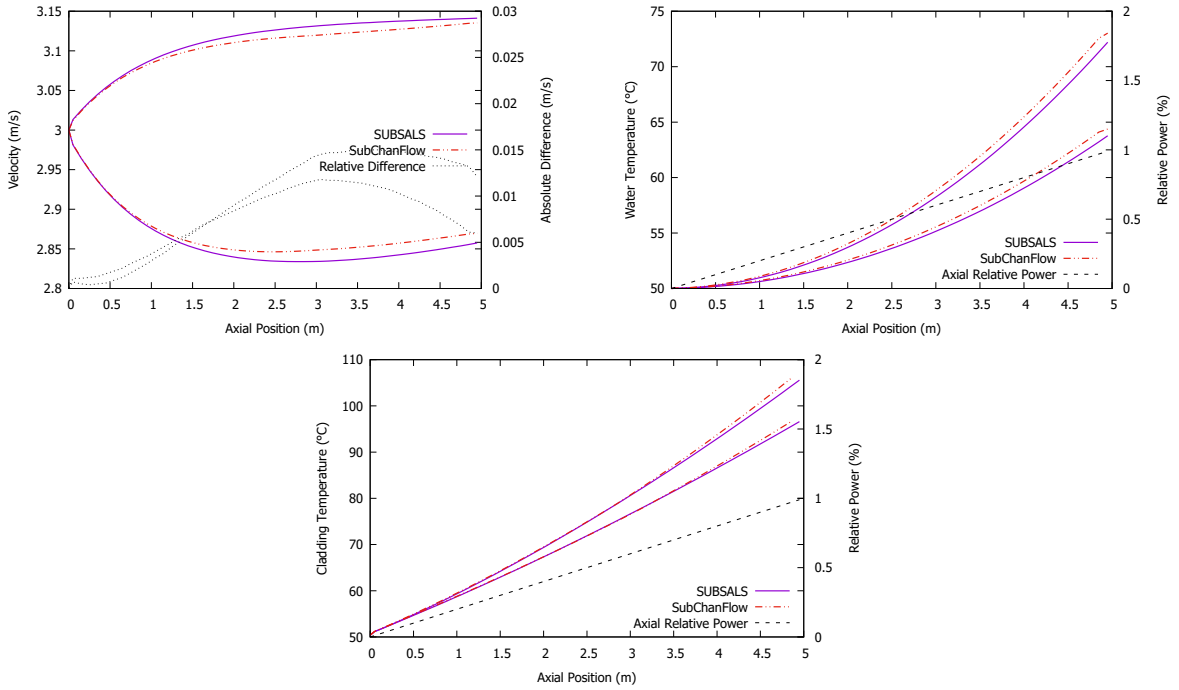

Figure 7. Comparison of axial velocity (top left), water temperature (top right) and cladding temperature (bottom) distribution calculations with linearly increasing axial power distribution.

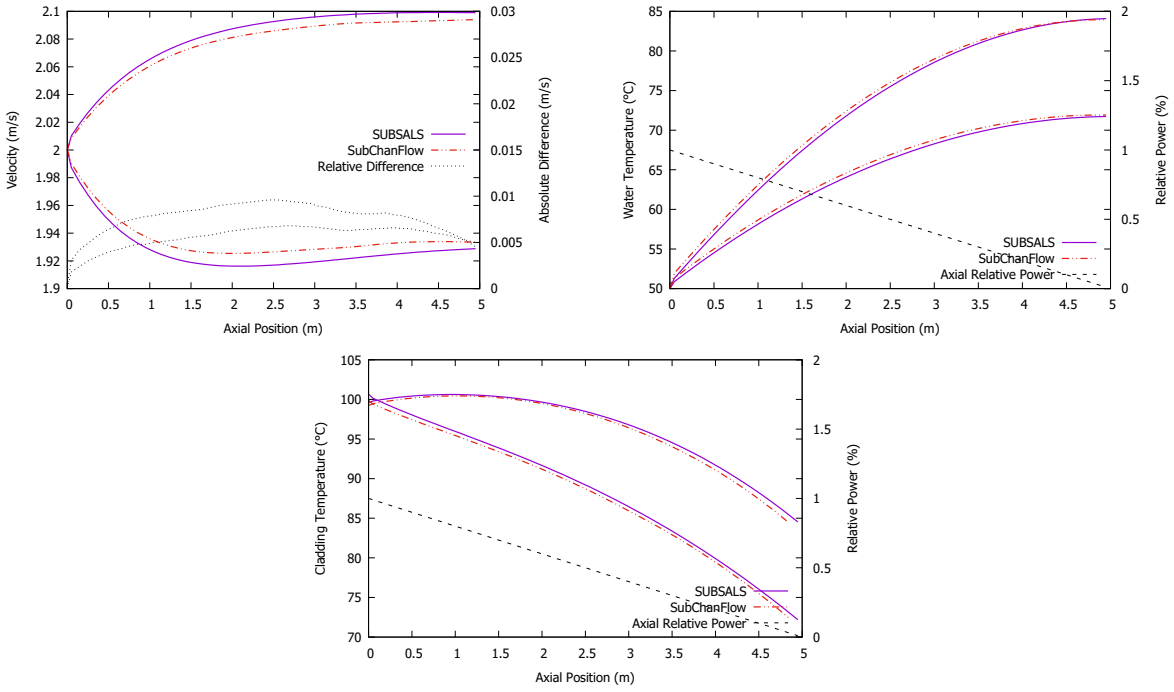

FIGURE 8. Comparison of axial velocity (top left), water temperature (top right) and cladding temperature (bottom) distribution calculations with linearly decreasing axial power distribution.

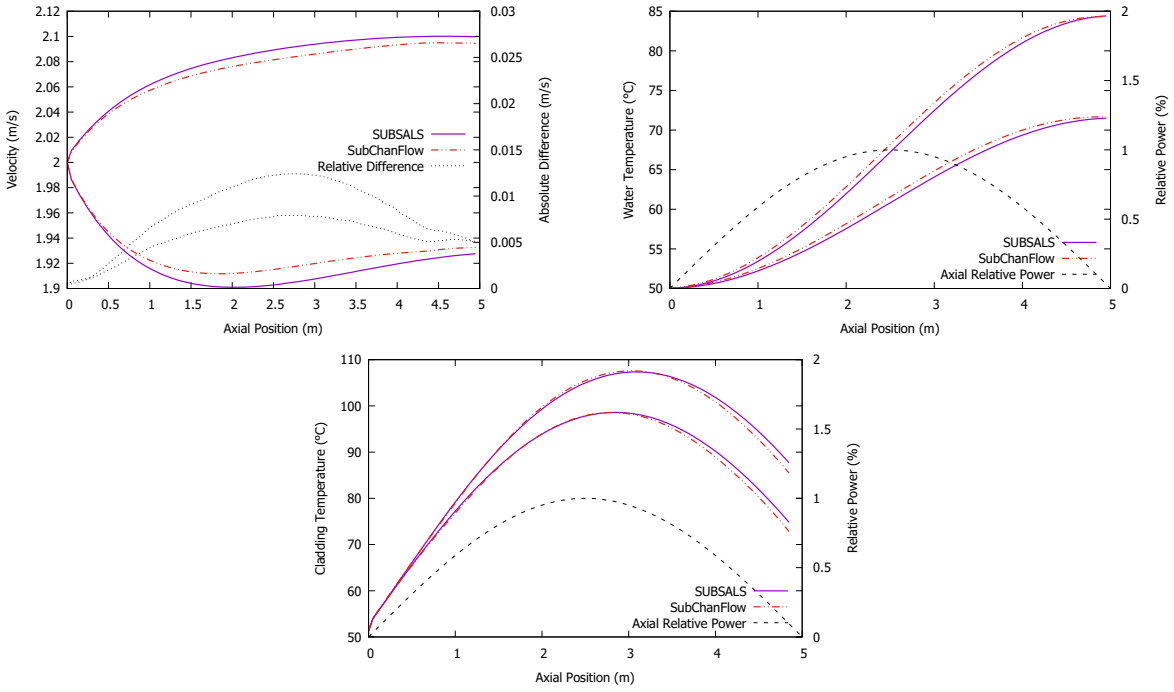

FIGURE 9. Comparison of axial velocity (top left), water temperature (top right) and cladding temperature (bottom) distribution calculations with sine axial power distribution.

Case	Inlet Velocity [m·s^{-1}]	Velocity Max. Error [m·s^{-1}]	Velocity RMSE [m·s^{-1}]	Water Temperature Max. Error [°C]	Water Temperature RMSE [°C]	Cladding Temperature Max. Error [°C]	Cladding Temperature RMSE [°C]
1	2	0.009	0.007	0.90	0.50	1.51	0.83
1	3	0.016	0.013	0.57	0.33	0.63	0.33
1	4	0.021	0.016	0.43	0.25	0.41	0.21
1	5	0.026	0.016	0.35	0.20	0.29	0.14
2	3	0.015	0.011	1.24	0.43	1.71	0.61
2	4	0.022	0.015	0.92	0.32	0.92	0.30
2	5	0.030	0.018	0.74	0.26	0.50	0.18
3	2	0.010	0.008	0.67	0.46	0.99	0.53
3	3	0.013	0.012	0.48	0.30	1.18	0.68
3	4	0.020	0.017	0.33	0.22	1.27	0.61
3	5	0.022	0.019	0.27	0.17	0.97	0.46
4	2	0.012	0.009	1.00	0.54	2.21	0.80
4	3	0.014	0.011	0.67	0.35	1.66	0.75
4	4	0.023	0.017	0.51	0.26	2.23	1.51
4	5	0.028	0.020	0.41	0.21	1.15	0.51

Table 2. Code-to-code comparison for different power profiles.

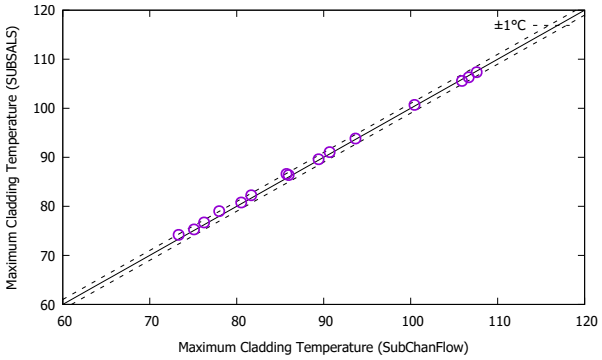

Figure 10. Comparison of maximum cladding temperature calculations.

is 1.51 °C and maximal peak cladding temperature error is 1.02 °C. Temperature RMSE decrease as the inlet velocity grows larger.

One of the most important steps in the qualification process of a new the thermal-hydraulic code is code-to-code comparison, especially when very few experimental data are available. Applicability of presented conclusions to the IRT type geometry, however, must be further investigated.

Attention needs to be paid to closure relations assessment, mainly turbulent mixing model. Furthermore, efforts are underway to develop experimental infrastructure for the thermal-hydraulic measurements and code validation at Research Centre Řež.

List of symbols

$\mathcal{A}$ Subchannel aspect ratio
d_h hydraulic diameter of subchannel [m]
f Darcy-Weisbach friction factor
$\mathcal{F}$ Turbulent transport correction factor
G Mass flux [kg·m^{-2}·s^{-1}]
g Acceleration due to gravity [m·s^{-2}]
h Specific enthalpy of water [J·kg^{-1}]
h^* Specific enthalpy in donor subchannel [J·kg^{-1}]
$K_\mathrm{trans.}$ Transverse flow pressure loss coefficient
l effective length of control volume for transversal flow [m]
P Power [W]
P_0 Total power generated in fuel assembly [W]
p Water pressure [Pa]
$_\mathrm{lin.}q$ Linear heat rate transferred to subchannel [W·m^{-1}]
$_\mathrm{surf.}q$ Heat flux to subchannel [W·m^{-2}]
S Subchannel flow area [m^2]
s Effective width of control volume for transversal flow [m]
$T_\mathrm{clad.}$ Cladding temperature [K]
T_∞ Bulk water temperature [K]
W Diversion crossflow [kg·m^{-1}·s^{-1}]
w Water velocity [m·s^{-1}]
w^* Water velocity in donor subchannel [m·s^{-1}]
w' Turbulent crossflow [kg·m^{-1}·s^{-1}]
Δz Length of axial node [m]

α Heat transfer coefficient [W·m^{-2}·K^{-1}]
β Turbulent factor
ε Surface roughness [m]
ϑ Fraction of heat transferred to coolant from whole fuel tube
λ_f Water conductivity [W·m^{-1}·K^{-1}]
μ Water dynamic viscosity [Pa·s]
ρ Water density [kg·m^{-3}]
ρ^* Water density in donor subchannel [kg·m^{-3}]
ϕ Normalized relative power

ax. Referring to axial nodalization.
az. Referring to azimuthal nodalization.
i Subchannel i
n Axial node n
rad. Referring to radial nodalization.

Nu Nusselt number
Pr Prandtl number
Re Reynolds number

References

[1] V. Nasonov, E. Ryazantsev, A. Taliev, A. Yashin. Water Velocity Determination in the Gaps of IRT-3M, -4M Fuel Assemblies. *Atomic Energy* **110**(389), 2011. https://doi.org/10.1007/s10512-011-9439-8.

[2] International Atomic Energy Agency. Research Reactor Database. [2022-06-30], https://nucleus.iaea.org/rrdb/#/home.

[3] F. Huet. LVR-15 Fuel Assembly Qualification Plan. Tech. rep., Technic Atome, 2020. [2022-06-30], https://ec.europa.eu/research/participants/documents/downloadPublic?documentIds=080166e5d575034a&appId=PPGMS.

[4] L. S. Tong, J. Weisman. *Thermal Analysis of Pressurized Water Reactors*. American Nuclear Society, La Grange Park, Illinois USA, 1996.

[5] M. Galassi, et al. GNU Scientific Library Reference Manual (3rd Ed.). [2022-06-30], ISBN 0954612078, http://www.gnu.org/software/gsl/.

[6] I. H. Bell, J. Wronski, S. Quoilin, V. Lemort. Pure and Pseudo-pure Fluid Thermophysical Property Evaluation and the Open-Source Thermophysical Property Library CoolProp. *Industrial & Engineering Chemistry Research* **53**(6):2498–2508, 2014. https://doi.org/10.1021/ie4033999.

[7] H. Blasius. Das Aehnlichkeitsgesetz bei Reibungsvorgängen in Flüssigkeiten. 1913. In: Mitteilungen über Forschungsarbeiten auf dem Gebiete des Ingenieurwesens, **131**:1–41, ISBN 978-3-662-01944-3, https://doi.org/10.1007/978-3-662-02239-9_1.

[8] D. J. Zigrang, N. D. Sylvester. A Review of Explicit Friction Factor Equations. *Journal of Energy Resources Technology* **107**(2):280–283, 1985. https://doi.org/10.1115/1.3231190.

[9] Information Systems Laboratories, Inc. RELAP5/MOD3 Code Manual. Volume 4, Models and Correlations. Tech. rep., 1995. https://doi.org/10.2172/106466.

[10] R. K. Salko, T. S. Blyth, et al. CTF Validation and Verification Manual. Tech. rep., 2016. https://doi.org/10.2172/1342678.

[11] D. S. Rowe. COBRA IIIC: Digital Computer Program for Steady State and Transient Thermal-hydraulic Analysis of Rod Bundle Nuclear Fuel Elements 1973. https://doi.org/10.2172/4480166.

[12] A. Liu, B.-W. Yang, B. Han, X. Zhu. Turbulent Mixing Models and Other Mixing Coefficients in Subchannel Codes—A Review Part A: Single Phase. *Nuclear Technology* **206**(9):1253–1295, 2020. https://doi.org/10.1080/00295450.2020.1792753.

[13] R. Pegonen, S. Bourdon, C. Gonnier, H. Anglart. An Improved Thermal-hydraulic Modeling of the Jules Horowitz Reactor Using the CATHARE2 System Code. *Nuclear Engineering and Design* **311**:156–166, 2017. https://doi.org/10.1016/j.nucengdes.2016.11.029.

[14] F. Dittus, L. Boelter. Heat Transfer in Automobile Radiators of the Tubular Type. *International Communications in Heat and Mass Transfer* **12**(1):3–22, 1985. https://doi.org/10.1016/0735-1933(85)90003-X.

[15] B. Petukhov. Heat Transfer and Friction in Turbulent Pipe Flow with Variable Physical Properties. vol. 6 of *Advances in Heat Transfer*, pp. 503–564. Elsevier, 1970. https://doi.org/10.1016/S0065-2717(08)70153-9.

[16] *Deterministic Safety Analysis for Nuclear Power Plants*. No. SSG-2 (Rev.1) in Specific Safety Guides. International Atomic Energy Agency, Vienna, 2019.